Nonlinear Dyn (2010) 60: 443–457
DOI 10.1007/s11071-009-9607-8

ORIGINAL PAPER

A new type of four-wing chaotic attractors in 3-D quadratic autonomous systems

Zenghui Wang · Guoyuan Qi · Yanxia Sun · Barend Jacobus van Wyk · Michaël Antonie van Wyk

Received: 25 March 2009 / Accepted: 2 October 2009 / Published online: 27 November 2009

Abstract In this paper, several smooth canonical 3-D continuous autonomous systems are proposed in terms of the coefficients of nonlinear terms. These systems are derived from the existing 3-D four-wing smooth continuous autonomous chaotic systems. These new systems are the simplest chaotic attractor systems which can exhibit four wings. They have the basic structure of the existing 3-D four-wing systems, which means they can be extended to the existing 3-D four-wing chaotic systems by adding some linear and/or quadratic terms. Two of these systems are analyzed. Although the two systems are similar to each other in structure, they are different in dynamics. One is sensitive to the initializations and sampling time, but another is not, which is shown by comparing Lyapunov exponents, bifurcation diagrams, and Poincaré maps.

Keywords Chaos · Four-wing chaotic attractor · Lyapunov exponents · Bifurcation · Poincaré map

Z. Wang (✉) · G. Qi · Y. Sun · B.J. van Wyk · M.A. van Wyk
French South African Technical Institute in Electronics (F'SATIE) & Department of Electrical Engineering, Tshwane University of Technology, Pretoria 0001, South Africa
e-mail: wangzengh@gmail.com

G. Qi
e-mail: guoyuanqi@gmail.com

Y. Sun
e-mail: sunyanxia@gmail.com

B.J. van Wyk
e-mail: vanwykb@gmail.com

Z. Wang
Department of Automation, Shandong University of Science and Technology, Qingao 266510, China

1 Introduction

Recently, it has been found that chaos is very useful in many application fields such as engineering, medicine, secure communications, and so on. Creating a chaotic system with a more complicated topological structure such as a multi-scroll or multi-wing attractor, therefore, becomes a desirable task and sometimes a key issue for many engineering applications. In this endeavor, there are two major thrusts: generalizing Chua's circuits with multi-scroll attractors and generalizing the Lorenz system with multi-wing attractors. Firstly, in the efforts of generalizing Chua's circuit [1] to produce multi-scroll attractors, several effective techniques have been developed, including some generalized Chua's circuits and cellular neural networks [2, 3]. In [1, 2, 4], the piecewise-linear (PWL) function method was utilized, which can increase the number of equilibria by adding breakpoints. A sine-function approach was then proposed for creating multi-scroll chaotic attractors [5]. Later, a stair function was used for generating 3D-grid-scroll attractors [6, 7]. More recently, several different nonlin-

ear functions including switching, hysteresis, and saturated functions were utilized for creating chaotic attractors with multi-merged basins of attraction, or with multi-scroll attractors [8–11]. Note that the aforementioned methods for generating multi-scroll attractors have some common characteristics [12, 13]:

(i) The nonlinearities of these systems are usually not smooth functions; they are either piecewise-linear continuous functions or discontinuous ones such as the stair function, switching function, and hysteresis-series function.
(ii) The basic techniques either increase the number of equilibria via PWL functions with more breakpoints, or use stair or hysteresis functions to realize equilibrium jumping.
(iii) The number of scrolls equals to that of the equilibria.
(iv) The basic shape of the attractors is cyclic, called scroll.

Secondly, another major thrust has been the generalization of the Lorenz system [14]. Recently, some new chaotic systems were proposed, including the Chen system, the generalized Lorenz system family, and the hyperbolic-type of generalized Lorenz canonical form [15–17]. Some four-dimensional chaotic systems were also presented, which have more complicated dynamic properties than three-dimensional chaotic systems, such as the system proposed in [18, 19]. It can be seen that the characteristics of generalized Chua's circuits are different from the generalized Lorenz systems. For example, the nonlinearities of these systems are usually smooth functions, the number of wings is not equal to the number of equilibria, and the basic shape of the attractors is a butterfly, called a 'wing' [12, 20].

In fact, most of the multi-scroll attractors were generated by increasing the breakpoints in the nonlinearity. Recently, a four-wing or a three-wing butterfly attractor was generated from a three-dimensional system [21] by relying on two embedded state-controlled binary switches. However, these systems are usually not smooth systems and the multi-wing or multi-scroll attractors might be viewed as the combination of several single scroll attractors by the varieties of parameters. It is desirable for a smooth quadratic autonomous system which produces multi-wing attractors and has a simple algebraic structure.

Since the discovery of the famous Lorenz chaotic system [29], continuous efforts have been devoted to seeking a unified theory and canonical forms for continuous-time 3-D autonomous quadratic chaotic systems [31]. Čelikovský and Vaněčk classified a generalized Lorenz system family using a condition associated with its linear part $A = [a_{ij}]$ [30, 31]; that is, the classic Lorenz system satisfies $a_{12}a_{21} > 0$, the Chen system [15] satisfies $a_{12}a_{21} < 0$ and the Lü system, which bridge the gap between the Lorenz system and the Chen system [32], satisfies $a_{12}a_{21} = 0$. It should be noted that such a simple algebraic classification does not indicate the holistic geometric structures of chaotic attractors and the formation mechanisms of chaos since the linear part of a dynamical system merely affects local properties of dynamical behaviors (e.g. the stability of equilibria) whereas chaos mainly results from the effect of its nonlinear parts. It would be better using nonlinear terms to classify chaotic systems, especially complex chaotic systems, such as the four wings chaotic systems.

In this paper, we firstly analyze several proposed smooth quadratic autonomous 4-wing chaos systems. Secondly, two canonical 3-D smooth continuous autonomous systems are proposed and analyzed which are derived from the existing 3-D four-wing smooth continuous autonomous chaotic systems. These new systems are the simplest chaotic attractor systems which can exhibit four wings. They have the basic structure of the existing 3-D four-wing systems, which means they can be extended to existing 3-D four-wing chaotic systems by adding some linear and/or quadratic terms. Although the two systems are similar to each other in structure, they are different in dynamics. Their differences are shown by the comparison of Lyapunov exponents, bifurcation diagrams, and Poincaré maps.

2 3-D four-wing smooth autonomous chaotic systems

In [22, 23], a three-dimensional smooth quadratic autonomous system which seemed to produce a four-wing attractor was proposed. At the beginning, it was believed that this system could produce a four-wing chaotic attractor, termed a "four-scroll attractor", but this was then later shown by the same authors to be a numerical artifact. It was not a real four-wing chaotic attractor but consisted of two co-existing and closely located double-wing attractors [24]. In [25], a 3-D autonomous quadratic system was reported, which can

generate a single four-scroll attractor. For the simplicity of comparison, the system is parameterized as

$$\begin{aligned}\dot{x}_1 &= a_1x_1 - y_1z_1 + a_2,\\ \dot{y}_1 &= b_1y_1 + x_1z_1,\\ \dot{z}_1 &= c_1z_1 + x_1y_1,\end{aligned} \tag{1}$$

where a_1, a_2, b_1, c_1 are real constants. If

$$\begin{cases} b_1c_1 > 0,\\ a_1 \neq 0,\\ a_1\sqrt{b_1c_1} < \min(-a_2, a_2) \quad \text{if } b_1 > 0,\\ a_1\sqrt{b_1c_1} > \max(-a_2, a_2) \quad \text{if } b_1 < 0,\end{cases}$$

there are five equilibria in this system, given by

$$S_0 = \left(-\frac{a_2}{a_1}, 0, 0\right),$$

$$S_{1,2} = \left(p, \pm\sqrt{\frac{(-a_2 - a_1p)b_1}{p}}p, \pm\sqrt{\frac{(-a_2 - a_1p)b_1}{p}}\right),$$

$$S_{3,4} = \left(-p, \mp\sqrt{\frac{(a_2 - a_1p)b_1}{p}}p, \pm\sqrt{\frac{(a_2 - a_1p)b_1}{p}}\right),$$

where $p = \sqrt{b_1c_1}$. As can be seen from the equilibria, there is no trivial equilibrium caused by the constant input of the first equation in (1). Consider the following transformation of variables:

$$x_1 = x_2 - \frac{a_2}{a_1}.$$

The system (1) can be reformulated as

$$\begin{aligned}\dot{x}_2 &= a_1x_2 - y_1z_1,\\ \dot{y}_1 &= b_1y_1 - \frac{a_2}{a_1}z_1 + x_2z_1,\\ \dot{z}_1 &= cz_1 - \frac{a_2}{a_1}y_1 + x_2y_1,\end{aligned} \tag{2}$$

which has a trivial equilibrium and is equivalent to system (1).

Another example is given by

$$\begin{aligned}\dot{x}_1 &= a_1x_1 + a_2y_1 + y_1z_1,\\ \dot{y}_1 &= b_2y_1 - x_1z_1 + b_{23}y_1z_1,\\ \dot{z}_1 &= c_3z_1 - x_1y_1.\end{aligned} \tag{3}$$

When $a_1 = 0.5$, $a_2 = 0.15$; $b_2 = -12.2$, $b_{23} = 1.0$, $c_3 = -8.79$, the system has a real four-scroll attractor with eight cross product terms on the right [26].

Qi [12] introduced a 3-D quadratic autonomous system

$$\begin{aligned}\dot{x}_1 &= a_1(y_1 - x_1) + e_1y_1z_1,\\ \dot{y}_1 &= c_1x_1 + d_1y_1 - x_1z_1,\\ \dot{z}_1 &= -b_1z_1 + x_1y_1,\end{aligned} \tag{4}$$

called the Qi 3-D four-wing system, which can generate two co-existing single-wing chaotic attractors and a pair of diagonal double-wing chaotic attractors. The system can also generate a four-wing chaotic attractor with very complicated topological structures over a large range of parameters.

Chen [27] presented a three-dimensional smooth quadratic autonomous chaotic system,

$$\begin{aligned}\dot{x}_1 &= a_1x_1 + ky_1 - y_1z_1,\\ \dot{y}_1 &= -b_1y_1 - z_1 + x_1z_1,\\ \dot{z}_1 &= -x_1 - c_1z_1 + x_1y_1,\end{aligned} \tag{5}$$

which can evolve into periodic and chaotic orbits in case of different parameters. When proper parameters are chosen, a single four-wing attractor and a single three-wing attractor appears.

Recently, Wang [28] presented a new three-dimensional smooth quadratic autonomous chaotic system,

$$\begin{aligned}\dot{x}_1 &= a_1(x_1 - y_1) - y_1z_1,\\ \dot{y}_1 &= -b_1 + x_1z_1,\\ \dot{z}_1 &= -c_1z_1 + d_1x_1,\end{aligned} \tag{6}$$

which can also show a single four-wing attractor and a single three-wing attractor.

As can be seen from systems (2), (3), (4), (5), and (6), these chaotic systems have similar features in common:

(1) There is at least one quadratic term in every equation, which means there is at least three quadratic terms in one system.
(2) There are five equilibria when these chaotic systems display four wings.
(3) There are at least three linear terms, and there is at least one linear term in every equation of these system.

The logical question is whether there is any system exhibiting similar behavior, however, it is simpler than these systems.

Based on the above features, a basic chaotic system[1]

$$\begin{aligned}\dot{x} &= ax + cyz,\\ \dot{y} &= dy - xz,\\ \dot{z} &= ez + fxy,\end{aligned} \tag{7}$$

is proposed which is likely to produce a four-wing chaotic attractor. Here, $a, c, d, e, f \in R$ are all constants, $cf \neq 0$ and x, y, z are the state variables. There are five equilibria in some places of the parameters space, e.g. $a = -14, c = 1, d = 16, e = -43, f = 1$. However, the following theorem shows that system (7) cannot exhibit a four-wing chaotic attractor.

Theorem 1 *System* (7) *cannot generate a four-wing chaotic attractor.*

Proof This theorem can be proved using different parameter space cases:

Case 1: $f < 0$

Consider the second and the third equations of (7), i.e.

$$\dot{y} = dy - xz, \tag{8}$$

$$\dot{z} = ez + fxy. \tag{9}$$

By multiplying both sides of (8) and (9) by fy and z, respectively, the two equations become

$$f\dot{y}y = dfy^2 - fxyz, \tag{10}$$

$$\dot{z}z = ez^2 + fxyz. \tag{11}$$

[1]Other kind of structure can convert into this system by simple linear transformation.

By adding both sides of (10) and (11), one obtains

$$f\dot{y}y + \dot{z}z = dfy^2 + ez^2. \tag{12}$$

Equation (12) is equivalent to

$$\frac{d(fy^2 + z^2)}{dt} = 2d\left(fy^2 + z^2\right) + (2e - 2d)z^2. \tag{13}$$

Solving the above equation yields

$$\begin{aligned}fy^2 + z^2 = e^{2dt}\Bigg(&\int_0^t e^{-2dt}(2e - 2d)z^2\,d\tau\\ &+ (fy_0^2 + z_0^2)\Bigg),\end{aligned} \tag{14}$$

where y_0 and z_0 are the initial state of system (7).
If $e > d$ and $\sqrt{-f}|y_0| < |z_0|$, according to (14), one obtains

$$fy^2 + z^2 > 0 \Rightarrow \sqrt{-f}|y| < |z|. \tag{15}$$

If $\sqrt{-f}|y_0| < |z_0|$ and $x_0 \neq 0$, then for any time $t > 0$, the system trajectory in the y–z plane will never travel from one domain $z > 0$ to another, $z < 0$, or vice versa. That is, if $z_0 > 0$, then there will always be $z(t) > 0$ for $t > 0$; if $z_0 < 0$, then there will always be $z(t) < 0$ for $t > 0$. The same is for $e < d$ and $\sqrt{-f}|y_0| > |z_0|$.

If the system can generate a four-wing attractor, then the attractor is ergodic and does not depend on the initial state, that is, the initial state value can be chosen arbitrarily, such as $\sqrt{-f}|y_0| < |z_0|$ or $\sqrt{-f}|y_0| > |z_0|$. It conflicts with the above analysis, so it is impossible to be a four-wing attractor when $f < 0$.

Case 2: $f > 0$

If $c > 0$, the same result can be got according to the first and third equations of system (7).

If $c < 0$, the same result can also be got according to the first and second equations of system (7).

The proof is thus complete. □

From Theorem 1, it is clear that if two or more quadratic term coefficients are either negative or positive at the same time then system (7) cannot generate a four wing chaotic attractor. Therefore, some linear or quadratic terms can be added to (7) which might cause it to exhibit a four-wing chaotic attractor if the added terms destroy the property proved by Theorem 1. Quadratic terms are very important in creating four-wing chaotic attractor and can be used to classify four-wing chaotic systems. In the following section,

several canonical four-wing chaotic attractors are proposed in 3-D quadratic autonomous systems according to the quadratic terms' coefficients.

3 3-D four-wing smooth autonomous canonical chaotic systems

Similar to the proof of Theorem 1, several systems, which might exhibit four-wing chaotic attractors, can be derived from system (7) by adding one or two linear terms.

If $f < 0$ and $c > 0$, the simplest way to break the condition which causes system (7) not to generate a four-wing chaotic attractor, is by adding a linear term to the second equation of system (7), e.g.

$$\begin{aligned} \dot{x} &= ax + cyz, \\ \dot{y} &= bx + dy - xz, \\ \dot{z} &= ez + fxy. \end{aligned} \tag{16}$$

If $f > 0$ and $c > 0$ (or $c < 0$), a linear term can be appended to the first equation of system (7) to form a new four-wing chaotic system, e.g.

$$\begin{aligned} \dot{x} &= ax + by + cyz, \\ \dot{y} &= dy - xz, \\ \dot{z} &= ez + fxy. \end{aligned} \tag{17}$$

If $f < 0$ and $c < 0$, at least two linear terms should be added to two equations of system (7) to violate the condition that makes system (7) not generate a four-wing chaotic attractor. There are many potential systems in this case. For example,

$$\begin{aligned} \dot{x} &= ax + b_1 y + cyz, \\ \dot{y} &= b_2 x + dy - xz, \\ \dot{z} &= ez + fxy, \end{aligned} \tag{18}$$

$$\begin{aligned} \dot{x} &= ax + b_1 y + cyz, \\ \dot{y} &= dy - xz, \\ \dot{z} &= b_2 y + ez + fxy, \end{aligned} \tag{19}$$

and so on.

As can be seen from Sect. 2, the coefficients of nonlinear terms in existing systems (2)–(5), which correspond to c and f in (7), meet condition $cf < 0$, that is, systems (2)–(5) can be derived from (16) and (17) by adding some linear and/or quadratic terms.

In this paper, we only focus on systems (16) and (17) to find similarities and differences. Systems (16) and (17) are not equivalent as the one cannot be changed to the other by a linear transformation if $b \neq 0$, and they are antithetic in some characteristics.

If systems (16) and (17) are dissipative, $\nabla V = \frac{\partial \dot{x}}{x} + \frac{\partial \dot{y}}{y} + \frac{\partial \dot{z}}{z} = a + d + e$ should be less than zero, that is, $a + d + e < 0$. It means a volume element V_0 is contracted by the flow into a volume element $V_0 e^{(a+d+e)t}$ in time t. For the dissipation of the two systems, parameters a, d, e should meet the same condition $a + d + e < 0$.

For distinction in the following analysis, systems (16) and (17) are rewritten as

$$\begin{aligned} \dot{x}_1 &= a_1 x_1 + c_1 y_1 z_1, \\ \dot{y}_1 &= b_1 x_1 + d_1 y_1 - x_1 z_1, \\ \dot{z}_1 &= e_1 z_1 + f_1 x_1 y_1, \end{aligned} \tag{20}$$

and

$$\begin{aligned} \dot{x}_2 &= a_2 x_2 + b_2 y_2 + c_2 y_2 z_2, \\ \dot{y}_2 &= d_2 y_2 - x_2 z_2, \\ \dot{z}_2 &= e_2 z_2 + f_2 x_2 y_2, \end{aligned} \tag{21}$$

where $a_1, b_1, c_1, d_1, e_1, a_2, b_2, c_2, d_2, e_2 \in R$, $f_1 \in R^-$ and $f_2 \in R^+$ are all constants and x_1, y_1, z_1, x_2, y_2, and z_2 are the state variables.

Remark 1 For system (20), the coefficients of quadratic terms are $f_1 < 0$ and $c_1 > 0$, however, for system (21), they are $f_2 > 0$ and $c_2 > 0$ (or $c_2 < 0$); system (20) cannot be transformed to system (21).

3.1 Equlibria

The equilibria of system (20) can be easily derived by solving the three equations $\dot{x}_1 = 0$, $\dot{y}_1 = 0$ and $\dot{z}_1 = 0$. There is one trivial equilibrium. Let

$$\begin{aligned} y_{1e} &= \sqrt{\frac{a_1 e_1}{c_1 f_1}}, \\ z_{1e}^1 &= \frac{b_1 c_1 + \frac{a_1}{|a_1|}\sqrt{b_1^2 c_1^2 - 4 a_1 c_1 d_1}}{2 c_1}, \\ z_{1e}^2 &= \frac{b_1 c_1 - \frac{a_1}{|a_1|}\sqrt{b_1^2 c_1^2 - 4 a_1 c_1 d_1}}{2 c_1}. \end{aligned} \tag{22}$$

If $\frac{a_1e_1}{c_1f_1} > 0, b_1^2c_1^2 - 4a_1c_1d_1 > 0$ and $c_1 \neq 0$, there are four nontrivial equilibria:

$$\begin{aligned} S_{1,2}^1 &= \left(\mp\frac{c_1}{a_1}y_{1e}z_{1e}^1, \pm y_{1e}, z_{1e}^1\right), \\ S_{3,4}^1 &= \left(\mp\frac{c_1}{a_1}y_{1e}z_{1e}^2, \pm y_{1e}, z_{1e}^2\right). \end{aligned} \tag{23}$$

The equilibria of system (21) can also be derived by solving the three equations $\dot{x}_2 = 0$, $\dot{y}_2 = 0$, and $\dot{z}_2 = 0$. There is one trivial equilibrium.

Let

$$\begin{aligned} x_{2e} &= \sqrt{-\frac{e_2d_2}{f_2}}, \\ z_{2e}^1 &= \frac{-b_2 + \sqrt{b_2^2 - 4a_2c_2d_2}}{2c_2}, \\ z_{2e}^2 &= \frac{-b_2 - \sqrt{b_2^2 - 4a_2c_2d_2}}{2c_2}. \end{aligned} \tag{24}$$

If $\frac{e_2d_2}{f_2} < 0, b_2^2 - 4a_2c_2d_2 > 0$, and $c_2 \neq 0$, there are four nontrivial equilibria:

$$\begin{aligned} S_{1,2}^2 &= \left(\pm x_{2e}, \pm\frac{1}{d_2}x_{2e}z_{2e}^1, z_{2e}^1\right), \\ S_{3,4}^2 &= \left(\pm x_{2e}, \pm\frac{1}{d_2}x_{2e}z_{2e}^2, z_{2e}^2\right). \end{aligned} \tag{25}$$

In this case, each of the systems has five equilibria (including the zero equilibrium). It means systems (20) and (21) are not topologically equivalent to the generalized Lorenz canonical form (GLCF) [17] which have three-equilibria at most.

Remark 2 There is no nontrivial equilibrium for both systems (20) and (21) in some parameter space, e.g. $\frac{a_1e_1}{c_1f_1} > 0$ or $b_1^2c_1^2 - 4a_1c_1d_1 > 0$ for system (20), and $\frac{e_2d_2}{f_2} < 0$ or $b_2^2 - 4a_2c_2d_2 > 0$ for system (21).

3.2 Simple property of the trivial equilibrium

By linearizing systems (20) and (21) at the origin (trivial equilibrium), one obtains the Jacobians,

$$J_0^1 = \begin{pmatrix} a_1 & 0 & 0 \\ b_1 & d_1 & 0 \\ 0 & 0 & e_1 \end{pmatrix}, \tag{26}$$

and

$$J_0^2 = \begin{pmatrix} a_2 & b_2 & 0 \\ 0 & d_2 & 0 \\ 0 & 0 & e_2 \end{pmatrix}, \tag{27}$$

respectively. The eigenvalues of matrices J_0^1 and J_0^2 are

$$\lambda_{01}^1 = a_1, \qquad \lambda_{02}^1 = d_1, \qquad \lambda_{03}^1 = e_1, \tag{28}$$

and

$$\lambda_{01}^2 = a_2, \qquad \lambda_{02}^2 = d_2, \qquad \lambda_{03}^2 = e_2, \tag{29}$$

respectively.

Remark 3 As $a_1, d_1, e_1, a_2, d_2, e_2 \in R$, there is no imaginary eigenvalue in (26) and (27); and a Hopf bifurcation does not exist near the trivial equilibrium for both systems (20) and (21).

3.3 Symmetry and similarity

It is obvious that systems (20) and (21) are symmetric about z-axis,which can be easily proven via the transformation $(x_1, y_1, z_1) \to (-x_2, -y_1, z_1)$ and $(x_2, y_2, z_2) \to (-x_2, -y_2, z_2)$, respectively. Equilibria S_1^1, S_2^1 (S_1^2, S_2^2) are also symmetric with respect to the z-axis and the same is for S_3^1, S_4^1 (S_3^2, S_4^2).

The dynamics near the neighborhood of S_1^1, S_2^1 is similar to each other in system (20), this also applies to S_3^1, S_4^1, which is caused by the similarity of the Jacobians of S_1^1 and S_2^1 (S_3^1 and S_4^1).

To prove this, let J_i^1 denote the Jacobian of $S_i^1, i = 1, \ldots, 4$, namely

$$J_1^1 = \begin{pmatrix} a_1 & c_1z_{1e}^1 & c_1y_{1e} \\ b_1 - z_{1e}^1 & d_1 & \frac{c_1}{a_1}y_{1e}z_{1e}^1 \\ f_1y_{1e} & -f_1\frac{c_1}{a_1}y_{1e}z_{1e}^1 & e_1 \end{pmatrix},$$

$$J_2^1 = \begin{pmatrix} a_1 & c_1z_{1e}^1 & -c_1y_{1e} \\ b_1 - z_{1e}^1 & d_1 & -\frac{c_1}{a_1}y_{1e}z_{1e}^1 \\ -f_1y_{1e} & f_1\frac{c_1}{a_1}y_{1e}z_{1e}^1 & e_1 \end{pmatrix},$$

$$J_3^1 = \begin{pmatrix} a_1 & c_1z_{1e}^2 & c_1y_{1e} \\ b_1 - z_{1e}^2 & d_1 & \frac{c_1}{a_1}y_{1e}z_{1e}^2 \\ f_1y_{1e} & -f_1\frac{c_1}{a_1}y_{1e}z_{1e}^2 & e_1 \end{pmatrix},$$

$$J_4^1 = \begin{pmatrix} a_1 & c_1 z_{1e}^2 & -c_1 y_{1e} \\ b_1 - z_{1e}^2 & d_1 & -\frac{c_1}{a_1} y_{1e} z_{1e}^2 \\ -f_1 y_{1e} & f_1 \frac{c_1}{a_1} y_{1e} z_{1e}^2 & e_1 \end{pmatrix}.$$

There is a transformation matrix T, such that

$$T^{-1} J_1^1 T = J_2^1, \qquad T^{-1} J_3^1 T = J_4^1, \tag{30}$$

where $T = \mathrm{diag}(-1\ -1\ 1)$, and T is an orthogonal matrix, since

$$T^{-1} = T^T = T. \tag{31}$$

Let $V_i^1 = [v_{i1}^1, v_{i2}^1, v_{i3}^1]$ be the matrix consisting of eigenvectors of $S_i^1, i = 1, \ldots, 4$; the following equations can then be obtained:

$$T^{-1} V_1^1 T = V_2^1, \qquad T^{-1} V_3^1 T = V_4^1. \tag{32}$$

Remark 4 $S_{1,2}^1$ and $S_{3,4}^1$ are two distinct equilibrium-pairs, and every equilibrium-pair has the same local stable, unstable, and center manifolds.

The same result can be obtained for system (21). From the above analysis, the local dynamics of (20) is similar to that of system (21) in some parameter spaces. The two canonical systems also have the same symmetry and similarity.

The spatial distribution and local dynamical linearized characteristics of the equilibria greatly influence the dynamics of the four wing systems. If the systems exhibit four wing chaotic attractors, the system equilibria $S_i, i = 1, 2, 3, 4$ are located at the centers of the four wings of the attractors, and the origin is the center of the whole chaotic attractor. Similar to the analysis in [12], these four equilibria $S_i, i = 1, 2, 3, 4$ should be symmetric with respect to the origin to some extent, and hence the effect of the four equilibria is also relatively balanced in space. It is essential condition to have five equilibria to ensure the system shows four wings according to the existing four-wing chaotic attractors in 3-D quadratic autonomous systems [12, 25–28].

4 The four-wing chaotic attractors

When $a_1 = 0.2, b_1 = -0.01, c_1 = 1, d_1 = -0.4, e_1 = -1$ and $f_1 = -1$, there are five equilibria in system (20):

$S_0^1 = (0, 0, 0)$,

$S_1^1 = (-0.6214, 0.4472, 0.2779)$,

$S_2^1 = (0.6214, -0.4472, 0.2779)$,

$S_3^1 = (0.6437, 0.4472, -0.2879)$,

$S_4^1 = (0.6214, -0.4472, -0.2879)$.

When $a_2 = -14, b_2 = 5, c_2 = 1, d_2 = 16, e_2 = -43$ and $f_2 = 1$, there are also five equilibria in system (21):

$S_0^2 = (0, 0, 0)$,

$S_1^2 = (26.2298, 20.7772, 12.6740)$,

$S_2^2 = (-26.2298, -20.7772, 12.6740)$,

$S_3^2 = (26.2298, -28.9740, -17.6740)$,

$S_4^2 = (-26.2298, 28.9740, -17.6740)$.

As $\nabla V_1 = \frac{\partial \dot{x_1}}{x_1} + \frac{\partial \dot{y_1}}{y_1} + \frac{\partial \dot{z_1}}{z_1} = a_1 + d_1 + e_1 = -1.2 < 0$ and $\nabla V_2 = \frac{\partial \dot{x_2}}{x_2} + \frac{\partial \dot{y_2}}{y_2} + \frac{\partial \dot{z_2}}{z_2} = a_2 + d_2 + e_2 = -41 < 0$, both systems (20) and (21) are dissipative. In order to investigate the stability of all the equilibria, we consider the Jacobian matrix with respect to each equilibrium and calculate their eigenvalues. The results are shown in Tables 1 and 2 for (20) and (21), respectively. Based on the eigenvalues, we know that the equilibria of systems (20) and (21) are all saddle-focus nodes implying that all the five equilibria are unstable.

With these parameter values, the corresponding Lyapunov exponents are $\lambda_1 = 0.064, \lambda_2 = 0$ and $\lambda_3 = -1.262$ for system (20); the fractional dimension is 2.05; and the system exhibits four-wing chaotic dynamics. The chaotic attractor is shown in Fig. 1. The projections of the phase portrait on the x_1–y_1, x_1–z_1, and y_1–z_1 planes are shown in Figs. 1(a)–1(c), respectively. The 3-D chaotic attractor is shown in Fig. 1(d).

When $a_2 = -14, b_2 = 5, c_2 = 1, d_2 = 16, e_2 = -43$, and $f_2 = 1$, the corresponding Lyapunov exponents are $\lambda_1 = 5.65, \lambda_2 = 0$, and $\lambda_3 = -46.6$ for system (21); the fractional dimension is 2.12; and the system exhibits four-wing chaotic dynamics. The chaotic attractor is shown in Fig. 2. The projections of the phase portrait on the x_2–y_2, x_2–z_2 and y_2–z_2 planes are shown in Figs. 1(a)–1(c), respectively. The 3-D chaotic attractor is shown in Fig. 1(d).

The systems' equilibria S_i^1 or $S_i^2, i = 1, \ldots, 4$, which are denoted by red '*', are located at the centers of the four wings of the attractor, and the origin

Table 1 Eigenvalues of Jacobian matrices for all equilibria in system (20)

S_0^1	S_1^1	S_2^1	S_3^1	S_4^1
$\lambda_1 = -0.4$	$\lambda_1 = -1.36$	$\lambda_1 = -1.36$	$\lambda_1 = -1.38$	$\lambda_1 = -1.38$
$\lambda_2 = 0.2$	$\lambda_{2,3} = 0.08 \pm 0.47i$	$\lambda_{2,3} = 0.08 \pm 0.47i$	$\lambda_{2,3} = 0.09 \pm 0.48i$	$\lambda_{2,3} = 0.09 \pm 0.48i$
$\lambda_3 = -1$				

Table 2 Eigenvalues of Jacobian matrices for all equilibria in system (21)

S_0^2	S_1^2	S_2^2	S_3^2	S_4^2
$\lambda_1 = -14$	$\lambda_1 = -50.56$	$\lambda_1 = -50.56$	$\lambda_1 = -58.52$	$\lambda_1 = -58.52$
$\lambda_2 = 16$	$\lambda_{2,3} = 4.78 \pm 25.12i$	$\lambda_{2,3} = 4.7839 \pm 25.12i$	$\lambda_{2,3} = 8.76 \pm 26.67i$	$\lambda_{2,3} = 8.76 \pm 26.67i$
$\lambda_3 = -43$				

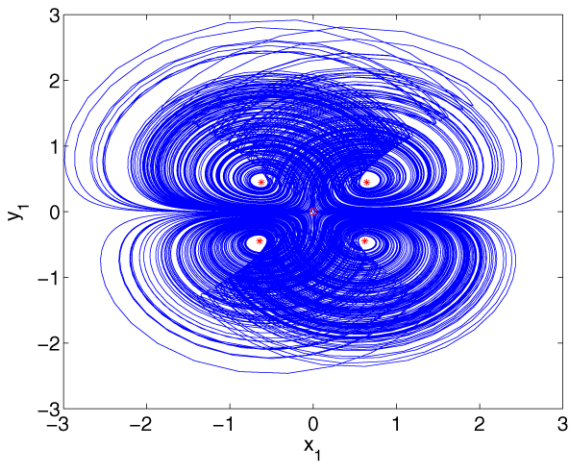

(a) Projection on the $x_1 - y_1$ plane

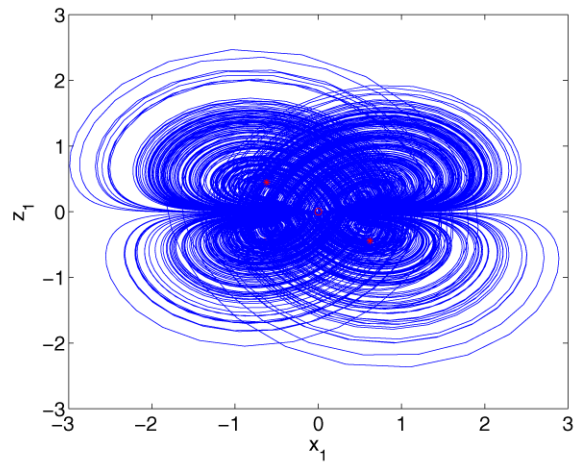

(b) Projection on the $x_1 - z_1$ plane

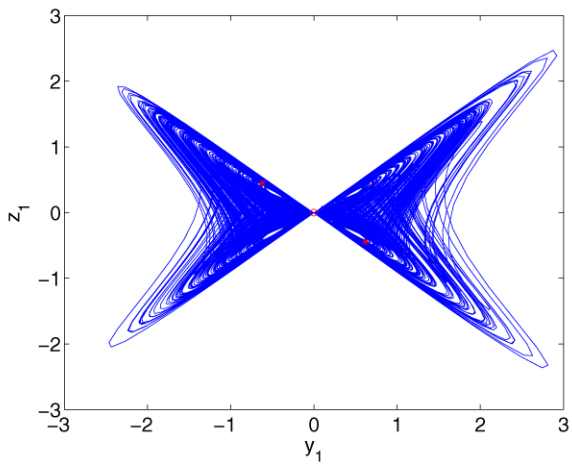

(c) Projection on the $y_1 - z_1$ plane

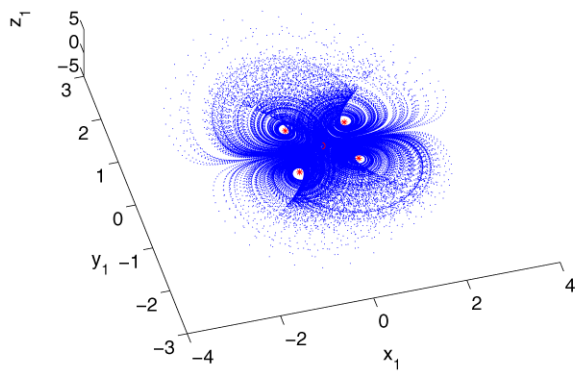

(d) 3-D view by '.' in the $x_1 - y_1 - z_1$ space

Fig. 1 Four-wing chaotic attractor of (20), with $a_1 = 0.2, b_1 = -0.01, c_1 = 1, d_1 = -0.4, e_1 = -1.0, f_1 = -1$

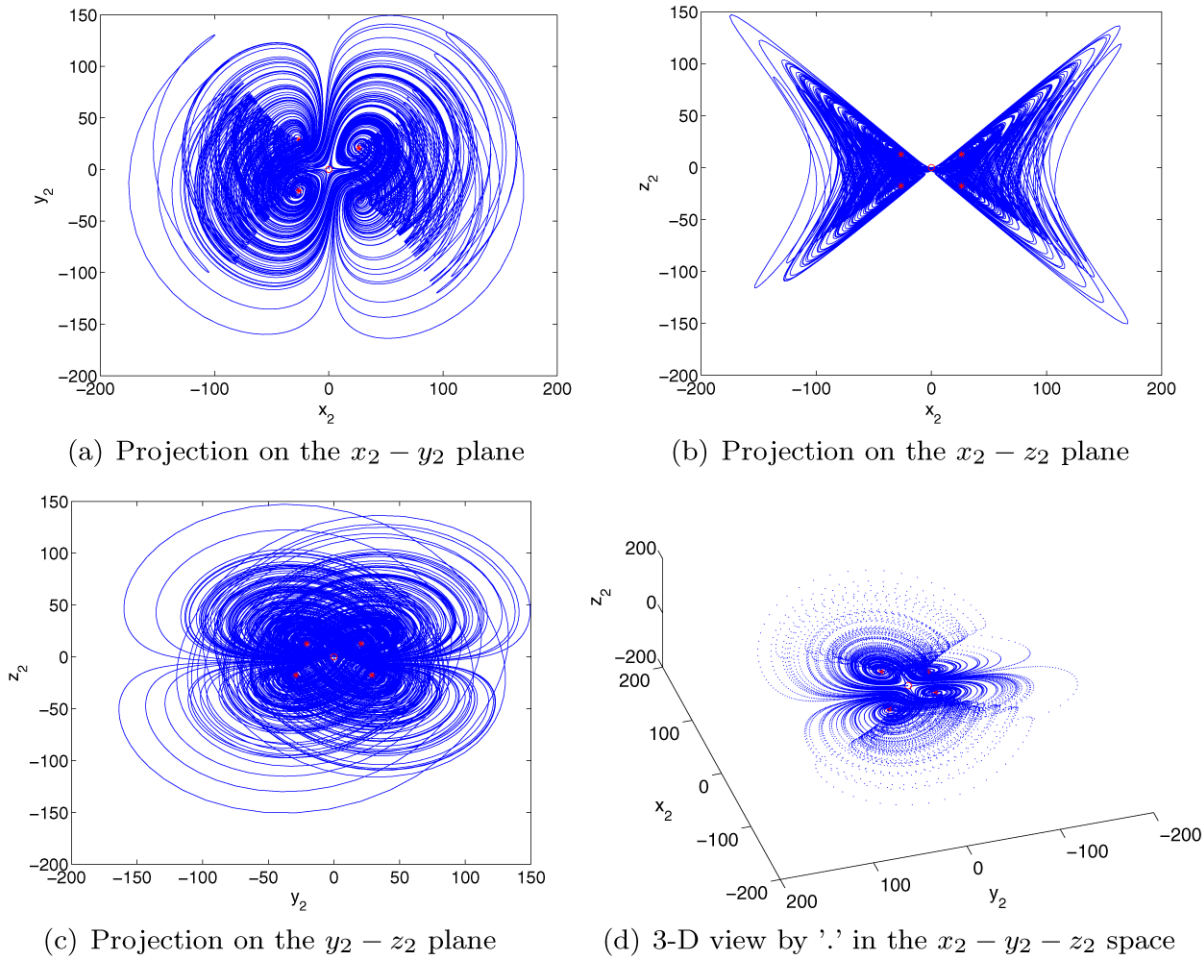

Fig. 2 Four-wing chaotic attractor of system (21), with $a_2 = -14$, $b_2 = 5$, $c_2 = 1$, $d_2 = 16$, $e_2 = -43$, $f_2 = 1$

is drawn as the red symbol 'o', which is in the center of the whole chaotic attractor shown in Figs. 1 and 2. It can be seen that there exist many orbits not only around $S^1_{1,2}$ ($S^2_{1,2}$), but also around $S^1_{3,4}$ ($S^2_{3,4}$), and even around $S^1_{1,3}$ and $S^1_{2,4}$ ($S^2_{1,3}$ and $S^2_{2,4}$), which play an important role in forming the real four-wing attractor, since they effectively connect the four sub-attractors, which surround the four equilibria.

Although the phase diagrams are similar to each other in Figs. 1 and 2, the details are different. The visible differences are Figs. 1(c) and 1(c), and Figs. 1(b) and 2(b). The shape in Fig. 1(c) is caused by adding $b_1 x$ to the second equation of (7). If $b_1 = 0$ and $e_1 < d_1$, the trajectory of system (20) will not cross the plane of $y_1 = 0$ which is the result of the proof of Theorem 1. As $b_1 = -0.01 \neq 0$, the trajectory of system (20) can across the plane of $y_1 = 0$ as shown in Fig. 1(c). The same result holds for system (21) in Fig. 1(b). The sensitivity of the two systems to initializations and sample time are also different which can be reflected by the time step used to calculate their states. For system (20), the time step can be chosen as 0.12 (s). The time step should be selected not larger than 0.001 (s) for system (21). However, the phase diagrams of the two systems are similar to each other as can be seen from Figs. 1 and 2.

4.1 System orbital bifurcation with respect to parameter b

As seen from Theorem 1, the parameter b (or b_1, b_2) is a very important factor to create a four-wing attractor.

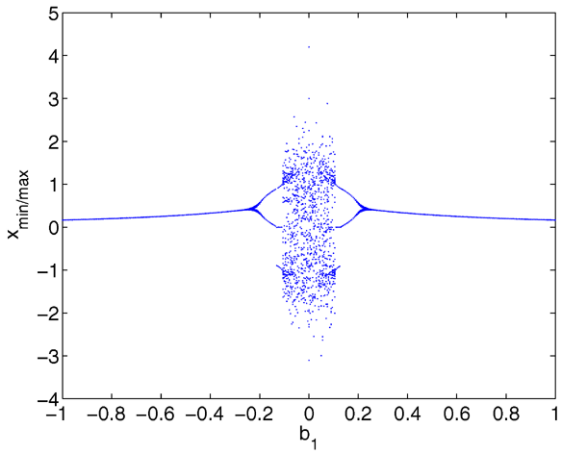

Fig. 3 The bifurcation diagram of the system (20) with respect to b_1, and with $a_1 = 0.2$, $c_1 = 1$, $d_1 = -0.4$, $e_1 = -1.0$, and $f_1 = -1$

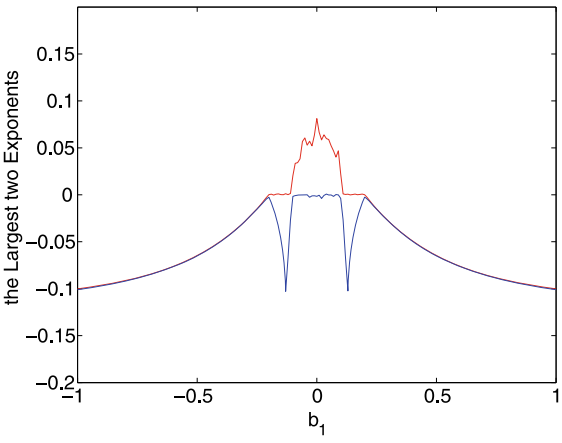

Fig. 4 The largest two Lyapunov exponent spectrum of the system (20) with respect to b_1, and with $a_1 = 0.2$, $c_1 = 1$, $d_1 = -0.4$, $e_1 = -1.0$, and $f_1 = -1$

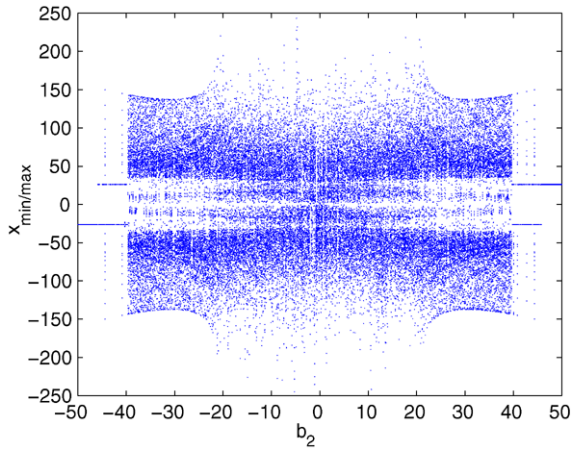

Fig. 5 The bifurcation diagram of the system (21) with respect to b_2, and with $a_2 = -14$, $c_2 = 1$, $d_2 = 16$, $e_2 = -43$, and $f_2 = 1$

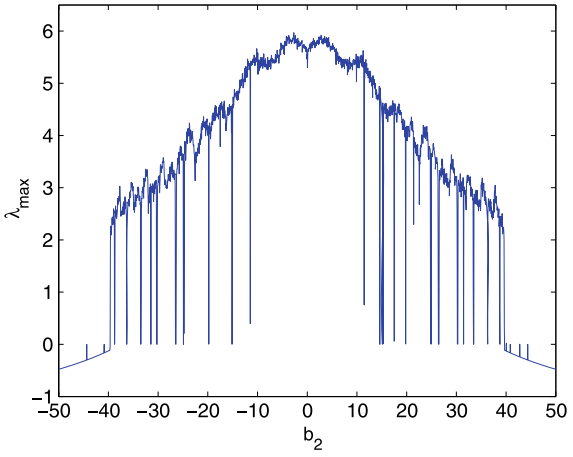

Fig. 6 The maximum Lyapunov exponent spectrum of the system (21) with respect to b_2, and with $a_2 = -14$, $c_2 = 1$, $d_2 = 16$, $e_2 = -43$, and $f_2 = 1$

Figure 3 shows the bifurcation diagram of the state variable x_1 of system (20), in which the orbit starts from (1, 1, 1). Figure 4 shows the maximum Lyapunov exponent spectrum, which corresponds directly to the bifurcation diagram shown in Fig. 3.

Figure 5 shows the bifurcation diagram of the state variable x_2 of system (21), in which the orbit starts from (1, 1, 1). Figure 6 shows the maximum Lyapunov exponent spectrum, which corresponds directly to the bifurcation diagram shown in Fig. 5.

Comparing Figs. 3 and 5 (or Figs. 4 and 6), system (21) can generate chaotic attractors over a large range of parameter b_2 which is wider than that of b_1 in system (20). Most of the largest Lyapunov exponents in system (20), which is less than 0.1, are smaller than the largest Lyapunov exponents in system (21) which are over 3. All of this means that system (21) is more sensitive than system (20).

There are two kinds of orbital dynamical attractors in systems (20) and (21), a local one and a global one. The local attractor relies on the initial region of the orbit, which includes a sink, some simple periodic orbits, and a single-wing chaotic attractor. The global attractor, which includes some complicated orbits around all equilibria, a double-wing chaotic attractor, and a four-wing chaotic attractor, does not rely on the initial re-

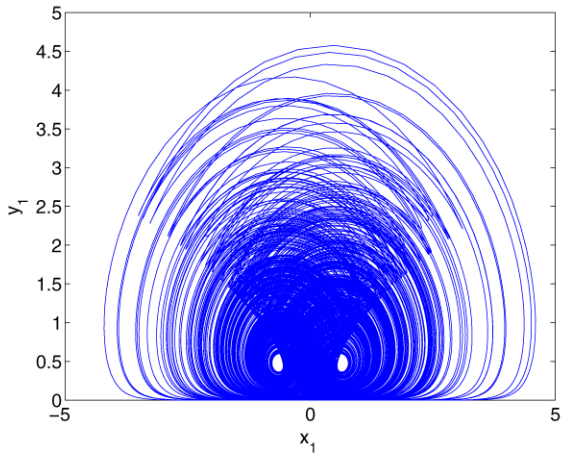

(a) Projection on the $x_1 - y_1$ plane with an initial state $(1, 1, 1)$

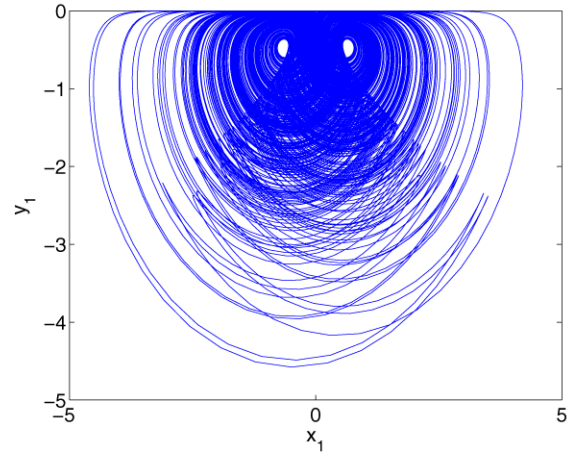

(b) Projection on the $x_1 - y_1$ plane with an initial state $(-1, -1, 1)$

Fig. 7 Double-wing chaotic attractor of (20), with $a_1 = 0.2$, $b_1 = 0$, $c_1 = 1$, $d_1 = -0.4$, $e_1 = -1.0$, and $f_1 = -1$

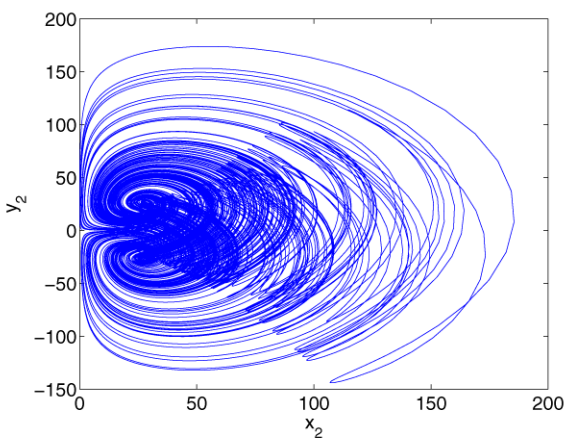

(a) Projection on the $x_2 - y_2$ plane with an initial state $(1, 1, 1)$

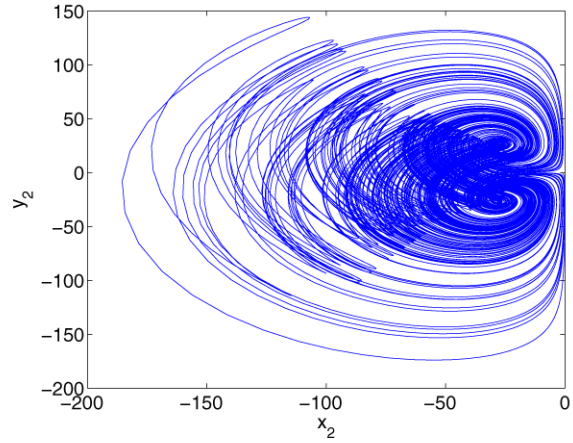

(b) Projection on the $x_2 - y_2$ plane with an initial state $(-1, -1, 1)$

Fig. 8 Double-wing chaotic attractor of system (21), with $a_2 = -14$, $b_2 = 0$, $c_2 = 1$, $d_2 = 16$, $e_2 = -43$, and $f_2 = 1$

gion of the orbit. An obvious illustration is the phase figures when $b = 0$ (or $b_1 = b_2 = 0$). When $a_1 = 0.2$, $b_1 = 0$, $c_1 = 1$, $d_1 = -0.4$, $e_1 = -1.0$, and $f_1 = -1$, the phase diagrams of (20) are shown in Fig. 7. In Fig. 7(a), the initial state is $(1, 1, 1)$ which is different from Fig. 7(b) with an initial state $(-1, -1, 1)$. When $a_2 = -14$, $b_2 = 0$, $c_2 = 1$, $d_2 = 16$, $e_2 = -43$ and $f_2 = 1$, the phase diagrams of (21) are shown in Fig. 8. In Fig. 8(a), the initial state is $(1, 1, 1)$ which is different from Fig. 8(b) with an initial state $(-1, -1, 1)$. As can be seen from Figs. 7 and 8, they cannot generate four-wing chaotic attractors when $b_1 = b_2 = 0$ satisfying Theorem 1, but create two co-existing double-wing chaotic attractors.

4.2 Poincaré map of the four-wing chaotic attractor

As an important analysis technique, the Poincaré map can reflect bifurcation and folding properties of chaos. When $a_1 = 0.2, b_1 = -0.01, c_1 = 1, d_1 = -0.4, e_1 = -1.0$, and $f_1 = -1$, one may take $x_1 = -0.62$, $y_1 = -0.45, z_1 = 0.28$ and $z_1 = 0$ as crossing planes, re-

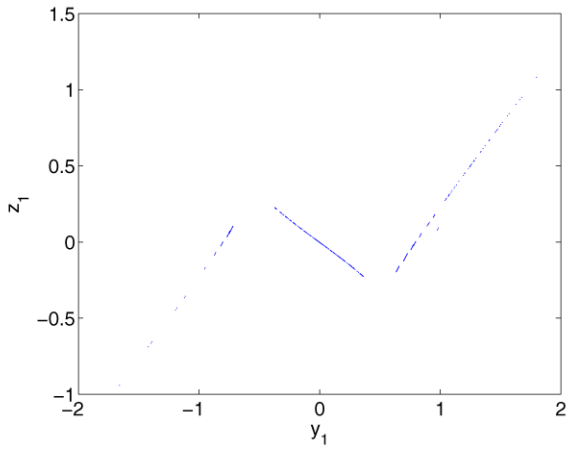

(a) Poincaré map on the crossing section $x_1 = -0.62$

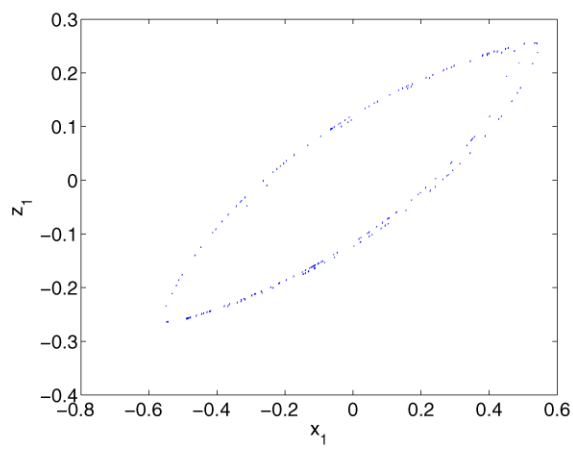

(b) Poincaré map on the crossing section $y_1 = -0.45$

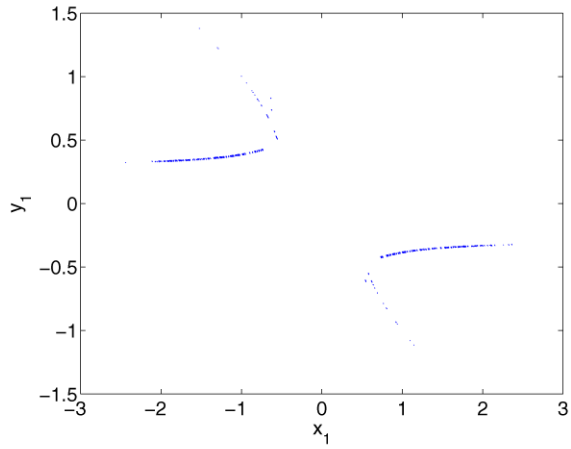

(c) Poincaré map on the crossing section $z_1 = 0.28$

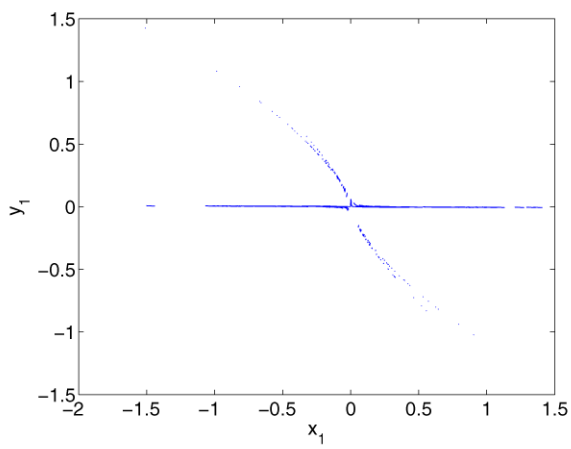

(d) Poincaré map on the crossing section $z_1 = 0$

Fig. 9 Four-wing chaotic attractor Poincaré mappings of system (20): with $a_1 = 0.2$, $b_1 = -0.01$, $c_1 = 1$, $d_1 = -0.4$, $e_1 = -1.0$, and $f_1 = -1$

spectively, where $x_1 = -0.62$, $y_1 = -0.45$ or $z_1 = 0.28$ is near the elements of the equilibrium of system (20).

When $a_2 = -14, b_2 = 5, c_2 = 1, d_2 = 16, e_2 = -43$, $f_2 = 1$, one may take $x_2 = -26.2$, $y_2 = -20.8$, $z_2 = 12.7$ and $z = 0$ as crossing planes, respectively, where $x_2 = -26.2$, $y_2 = -20.8$ or $z_2 = 12.7$ is near the elements of the equilibrium of system (21). Figures 9 and 10 show the Poincaré mapping on several sections, with several sheets of the attractors visualized. It is clear that some sheets are folded, which indicates that the systems have extremely rich dynamics.

Although the orientations and some details are different, by comparing Figs. 9 and 10, we can find that the shape of Fig. 9(a) is similar to Fig. 10(b), Fig. 9(b) is like Fig. 10(a), and Figs. 9(c) and (c) are similar to Figs. 10(c) and (d), respectively. These Poincaré maps reveal that the two canonical four-wing chaotic systems can generate similar four-wing chaotic attractors in the geometrical view.

4.3 Frequency spectral analysis

Frequency spectra can be used to analyze chaotic attractors since they can reveal how random signals are. The frequency spectra of signals, generated numeri-

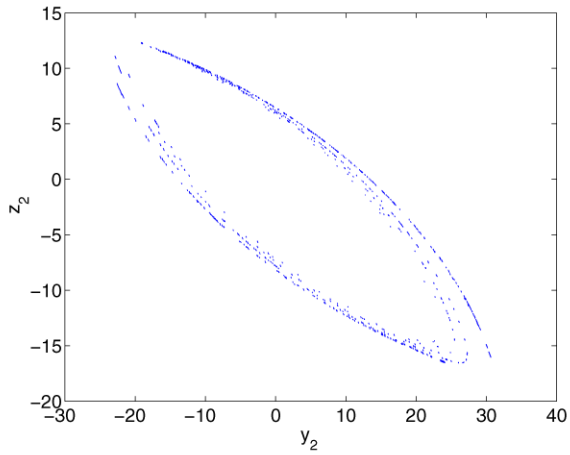

(a) Poincaré map on the crossing section $x_2 = -26.2$

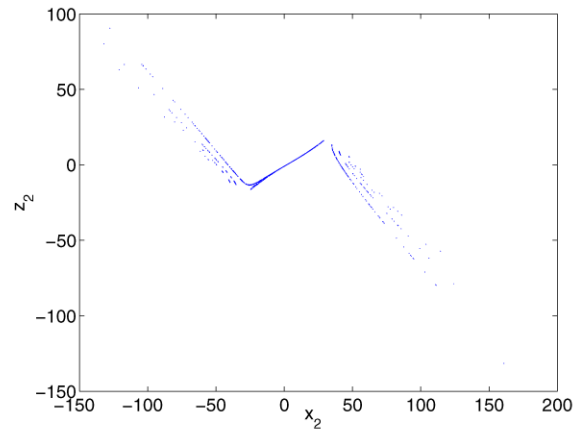

(b) Poincaré map on the crossing section $y_2 = -20.8$

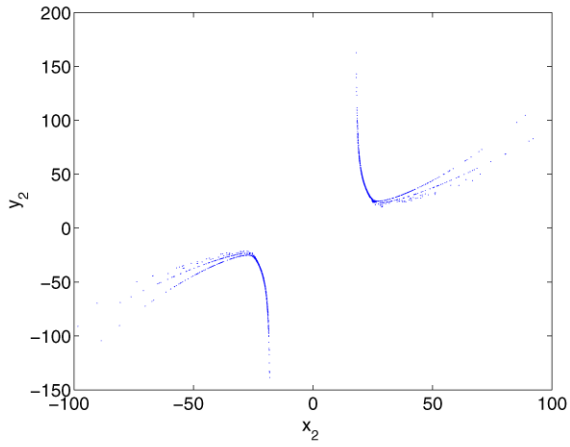

(c) Poincaré map on the crossing section $z_2 = 12.7$

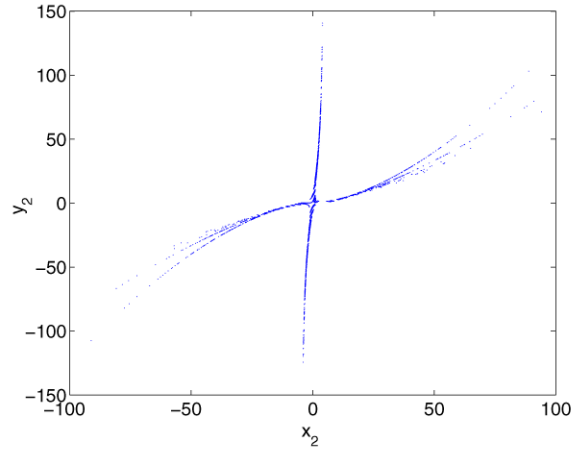

(d) Poincaré map on the crossing section $z_2 = 0$

Fig. 10 Four-wing chaotic attractor Poincaré mappings of system (21): with $a_2 = -14$, $b_2 = 5$, $c_2 = 1$, $d_2 = 16$, $e_2 = -43$, $f_2 = 1$

cally from the four-wing chaotic systems (20) and (21) proposed in this paper, are shown in Figs. 11 and 12, respectively. For calculation, the Runge–Kutta method was used to solve all systems, with sampling time step 0.01 (s) and 0.001 (s), running time 0–500 (s), the number of spectral averages 3, and all spectra are normalized. Note that the bandwidths of signals y_2 and z_2 are over 22 Hz band, which is wider than the bandwidths of system (20) with a bandwidth of 0.9 Hz. It shows that system (21) is more random and disorder than system (20) which also means (21) is more sensitive than (20).

5 Conclusion

Through the analysis of several 3-D four-wing smooth quadratic autonomous chaotic systems, it was found that these systems have similar features related to the creation of four-wing chaotic attractors. Two canonical 3-D continuous autonomous systems, which are distinct with each other in dynamics, were consequently introduced and analyzed. Lyapunov exponents, bifurcation diagrams, and Poincaré maps showed that the dynamics of these two systems are different despite of similar geometrical structure. The two simpler systems are very convenient to investigate the dynamical behavior of multi-wing chaotic systems.

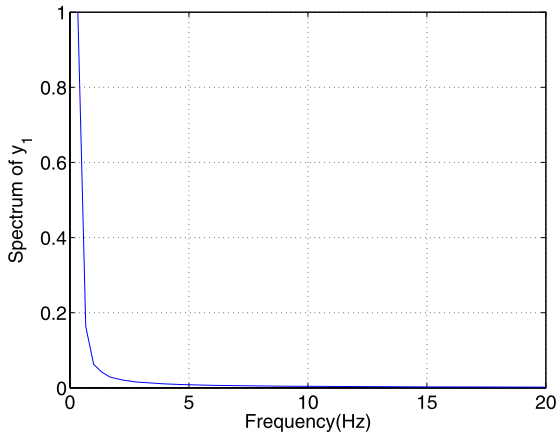

(a) The signal of variable y_1.

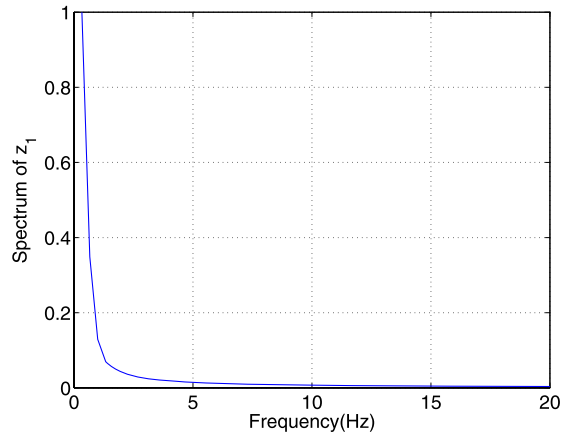

(b) Two the signal of variable z_1.

Fig. 11 The frequency spectra generated numerically from the proposed four-wing chaotic system (20), with $a_1 = 0.2$, $b_1 = -0.01$, $c_1 = 1$, $d_1 = -0.4$, $e_1 = -1.0$, and $f_1 = -1$

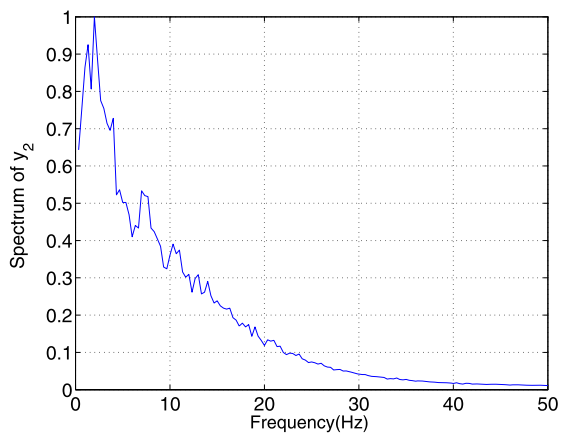

(a) The signal of variable y_2.

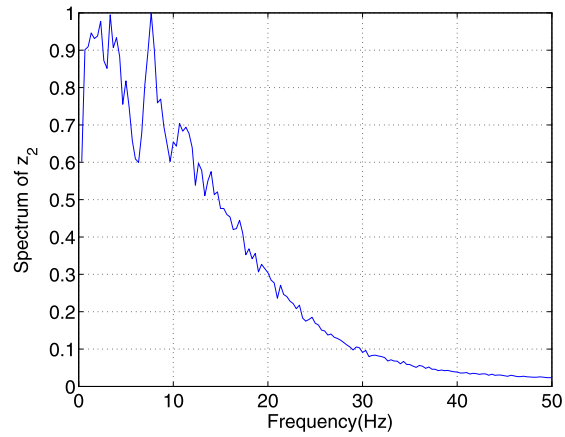

(b) Two the signal of variable z_2.

Fig. 12 The frequency spectra generated numerically from the proposed four-wing chaotic system (21), with $a_2 = -14$, $b_2 = 5$, $c_2 = 1$, $d_2 = 16$, $e_2 = -43$ and $f_2 = 1$

Acknowledgements This work was supported by the grants: Tshwane University Research foundation, South Africa; the Natural Science Foundation of China (Nos. 10772135, 60774088) and the Scientific Foundation of Tianjin City, China (No. 07JCY-BJC05800).

References

1. Chua, L.O., Komuro, M., Matsumoto, T.: The double scroll family. IEEE Trans. Circuits Syst. I **33**, 1072–1178 (1986)
2. Chua, L.O., Roska, T.: The CNN paradigm. IEEE. Trans. Circuits Syst. I C **40**, 147–156 (1993)
3. Suykens, J.A.K., Chua, L.O.: n-double scroll hypercubes in 1-D CNNs. Int. J. Bifurc. Chaos **7**, 1873–1885 (1997)
4. Suykens, J.A.K., Vandewalle, J.: Generation of n-double scrolls ($n = 1; 2; 3; 4; \ldots$). IEEE Trans. Circuits Syst. I **40**, 861–867 (1993)
5. Tang, K.S., Zhong, G.Q., Chen, G., Man, K.F.: Generation of n-scroll attractors via sine function. IEEE Trans. Circuits Syst. I **48**, 1369–1372 (2001)
6. Yalcin, M.E., Ozoguz, S., Suykens, J.A.K., Vandewalle, J.: n-scroll chaos generators: a simple circuit model. Electron. Lett. **37**, 147–148 (2001)
7. Yalcin, M.E., Suykens, J.A.K., Vandewalle, J., Ozoguz, S.: Families of scroll grid attractors. Int. J. Bifurc. Chaos **12**, 23–41 (2002)
8. Lü, J., Yu, X., Chen, G.: Generating chaotic attractors with multiple merged basins of attraction: a switching

piecewise-linear control approach. IEEE Trans. Circuits Syst. I **50**, 198–207 (2003)
9. Lü, J., Han, F., Yu, X., Chen, G.: Generating 3-D multi-scroll chaotic attractors: a hysteresis series switching method. Automatica **40**, 1677–1687 (2004)
10. Lü, J., Chen, G., Yu, X.: Design and analysis of multi-scroll chaotic attractors from saturated function series. IEEE Trans. Circuits Syst. I **51**, 2476–2490 (1999)
11. Han, F., Yu, X., Lü, J., Chen, G., Feng, Y.: Generating multi-scroll chaotic attractors via a linear second-order hysteresis system. Dyn. Contin. Discrete Impulse Syst. Ser B, Appl. Algorithms **12**, 95–110 (2005)
12. Qi, G.Y., Chen, G.R., van Wyk, M.A., van Wyk, B.J., et al.: A four-wing attractor generated from a new 3-D quadratic autonomous system. Chaos Solitons Fractals **38**, 705–721 (2008)
13. Qi, G.Y., Chen, G., Li, S.W., Zhang, Y.H.: Four-wing attractors: from pseudo to real. Int. J. Bifurc. Chaos **16**, 859–885 (2006)
14. Vaneček, A., Čelikovský, S.: Control Systems from Linear Analysis to Synthesis of Chaos. Prentice-Hall, London (1996)
15. Chen, G., Ueta, T.: Yet another chaotic attractor. Int J. Bifurc. Chaos **9**, 1465–1466 (1999)
16. Chen, G., Lü, J.: Dynamical Analysis, Control and Synchronization of the Generalized Lorenz Systems Family. Science Press, Beijing (2003) (in Chinese)
17. Čelikovský, S., Chen, G.: On the generalized Lorenz canonical form. Chaos Solitons Fractals **26**, 1271–1276 (2005)
18. Qi, G.Y., Du, S.Z., Chen, G., Chen, Z.Q., Yuan, Z.Z.: On a four-dimensional chaotic system. Chaos Solitons Fractals **23**, 1671–1676 (2005)
19. Qi, G.Y., Chen, G.R., Zhang, Y.H.: Analysis and circuit implementation of a new 4-D chaotic system. Phys. Lett. A **352**, 386–397 (2006)
20. Qi, G.Y., Barend, J., Michael, A.: A four-wing attractor and its analysis. Chaos Solitons Fractals **40**, 2016–2030 (2009)
21. Elwakil, A.S., Özoğz, S., Kennedy, M.P.: A four-wing butterfly attractor from a fully autonomous system. Int. J. Bifurc. Chaos **13**, 3093–3098 (2003)
22. Liu, W.B., Chen, G.: A new chaotic system and its generation. Int. J. Bifurc. Chaos **13**, 261–266 (2003)
23. Liu, W.B., Chen, G.: Dynamical analysis of a chaotic system with two double-scroll chaotic attractors. Int. J. Bifurc. Chaos **14**, 971–998 (2004)
24. Liu, W.B., Chen, G.: Can a three-dimensional smooth autonomous quadratic chaotic system generate a single four-scroll attractor? Int. J. Bifurc. Chaos **14**, 1395–1403 (2004)
25. Lü, J.: A new chaotic system and beyond: the generalized Lorenz-like system. Int. J. Bifurc. Chaos **14**, 1507–1537 (2004)
26. Zhou, T.S., Chen, G.: Classification of chaos in 3-D automations quadratic system, I: basic framework and methods. Int. J. Bifurc. Chaos **16**, 2459–2479 (2006)
27. Chen, Z., Yang, Y., Yuan, Z.: A single three-wing or four-wing chaotic attractor generated from a three-dimensional smooth quadratic autonomous system. Chaos Solitons Fractals **38**, 1187–1196 (2008)
28. Wang, L.: 3-scroll and 4-scroll chaotic attractors generated from a new 3-D quadratic autonomous system. Nonlinear Dyn. (2008). doi:10.1007/s11071-008-9417-4
29. Lorenz, E.N.: Deterministic non-periodic flow. J. Atmos. Sci. **20**, 130–141 (1963)
30. Čelikovský, S., Vaněček, A.: Bilinear systems and chaos. Kybernetika **30**, 403–424 (1994)
31. Čelikovský, S., Chen, G.: On a generalized Lorenz canonical form of chaotic systems. Int. J. Bifurc. Chaos **12**, 1789–1812 (2002)
32. Lü, J., Chen, G., Cheng, D., Čelikovský, S.: Bridge the gap between the Lorenz system and the Chen system. Int J. Bifurc. Chaos **12**, 2917–2928 (2002)